

A Study On The Cracking Behavior Of Gfrp Reinforced Concrete Beams

Enio Deneko¹ and Esmerald Filaj²

¹Department of Mechanics of Structures
Faculty of Civil Engineering, Polytechnic Faculty of Tirana
Tirana, Albania
eniodeneko@hotmail.com

²Department of Building Construction and Transport Infrastructure
Faculty of Civil Engineering, Polytechnic Faculty of Tirana
Tirana, Albania
e_filaj@yahoo.com



Abstract — During the last years, the use of GFRP bars as internal reinforcement in concrete structures, gained more and more attention, as a good and sometimes a better alternative to steel reinforcement especially in corrosive situations and in aggressive environment. GFRP bars, which are fibers with high resistance immersed in a polymer resin matrix, with high tensile resistance and also resistant to corrosion, give better results regarding the tensile strength of the concrete structures, but due to their low elastic modulus and the poor bond with the concrete, as compared to steel reinforcing bars, the use of GFRP results in greater deflections and larger crack width under service loads.

This paper aims to investigate the cracking behavior of GFRP reinforced members and their design based on SLS method as it represents the most problematic one, focusing on the cracking of GFRP reinforced beams. The work presented here includes the results from 4 GFRP beams tested. During the loading the cracks visible to the naked eye were marked with a pencil and photographed, creating a complete framework of the crack development in the beams until their destruction. The data related to the size of the cracks, the reductions, and the curvature of the beam as a function of loading, are recorded by the MGC device and elaborated in the form of graphs. Experimental data were analyzed and integrated in appropriate charts and are compared to predicted calculations based on American Code ACI 440.1R -06.

Keywords — GFRP, GFRP-RC beams, concrete, SLS design, crack width, crack spacing.

I. INTRODUCTION

FRP bars can be effectively used in corrosive environments. The problems seem similar to steel reinforced concrete, but limits and analytic models are different, because of the many types of GFRP bars on the market, with a large variety of mechanical characteristics. GFRP bars display a linear elastic behavior up to the point of failure and do not demonstrate ductility. GFRP has a lower elastic modulus than steel bars, only 20-25% of the steel bars. Also the bond strength of FRP bars and concrete is lower than that of steel bars, leading to an increase in the depth of cracking, a decrease in stiffening effect, and so an increase of the deflection of the beams compared to an equivalent cross-section of reinforcement of steel reinforced concrete beams [4], [7].

Because of it, the deflection criterion may control the design GFRP reinforced beams. In service conditions, structural concrete elements reinforced with FRP bars operate at between 20 and 40% of their flexural capacity [3], [4], [5], [6].

II. METHODOLOGY

Glass fibers (GFRP) are used as reinforcing bars instead of steel reinforcement, as external reinforcing sheets and structural profiles. They suffer the effect of cracks, resistance loss and rupture and under loading. They have very high tensile strength, but are much brittle than steel bars, showing no yielding properties.

Glass fibers (GFRP), are among the most common of FRP bars and they are offered by a large number of manufacturers in the world. Their size range from 3/8 to 1 3/8 in. (9 – 41 mm).

The service conditions also depend on the importance of the structure and the environment. The permitted crack widths for these elements are not the same as for conventional concrete elements reinforced with steel bars, due to the greater corrosion resistance of GFRP bars. The application of GFRP-RC to beams reinforced with FRP reinforcing bars is being investigated to find possible improvements to maximum crack widths. This is only one of a major number of experimental investigations carried out by many researchers. The research provides quantitative and comparative data with predicted crack width responses of GFRP beams. The comparison is made based on the American Code (ACI-440R-96).

1. Cracking of gfrp-rc beams under service loads

Restrictions on the maximum crack width under the action of service loads, for GFRP reinforced concrete, are needed to control the penetration of liquids that can degrade the bars, as well as to protect the most aesthetic appearance of the elements. Although not technically unsafe, large cracks can create discomfort in people, due to their perception as a structural collapse. The maximum crack widths recommended by ACI 440.1R-06 code are given in Table 1 along with the allowable cracks for steel-reinforced concrete members according to ACI 318-95 code.

Table 1. Permissible crack width of concrete members

| Exposure conditions | Concrete reinforcement in mm. (in.) | |
|---------------------|-------------------------------------|-------------|
| External | 0.5 (0.020) | 0.3 (0.013) |
| Internal | 0.7 (0.028) | 0.4 (0.016) |

It should be said that since ACI 318-99 code, the exact calculation of cracks for steel-reinforced concrete members is not required anymore for these elements, but an approximate method is used, based on bar spacing in the cross-section of the member and the stresses induced by the service loads. In the elements reinforced with GFRP bars, due to the low bending stiffness and high tensile strength of GFRP, it is recommended to correctly define the crack width. In Table 2, are given the permissible crack width for GFRP-RC beams based on different design codes.

Table 2. Permissible crack width for GFRP-RC beams based on different design codes

| CODE | EXPOSURE | W _{max} (mm) |
|------------|----------------------|-----------------------|
| JSCE | | 0.51 |
| CSA | Internal | 0.71 |
| CSA | External | 0.51 |
| EUROCRETE | Waterproof | 0.2 |
| EUROCRETE | Aesthetic | 0.3 - 0.5 |
| EUROCRETE | Structural integrity | 0.5 – 1.0 |
| ACI | Internal | 0.7 |
| ACI | External | 0.5 |
| EUROCODE 2 | | 0.5 |

FRP bars are resistant to corrosion, so the permissible crack width is greater than for steel bars, when corrosion is a major problem, but in addition there are other factors that determine the allowed crack width, such as the visual effect (aesthetic) and the shear forces. These restrictions are not enough for structures exposed to aggressive environments or when those should be waterproof.

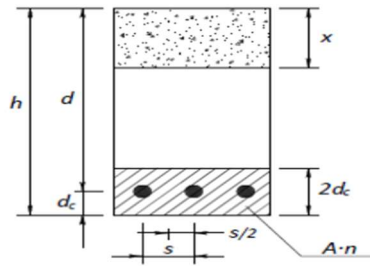


Fig. 1. Parameters for calculating the crack width

ACI 318R-95, used empirical formulations, based on Gergely & Lutz (1968), to calculate the maximum crack width in concrete beams and in thick one-way slabs. The simplified equation for the most probable crack width at tensile face of the beam:

$$w = 2.2 \cdot \beta \cdot \epsilon_s \sqrt[3]{d_c \cdot A} \tag{1}$$

ϵ_s – the strain in the steel reinforcement at the cracked section

d_c – the concrete cover measured from the centroid of tension reinforcement to the extreme tension face of the concrete.

A – effective tension area of the concrete around the flexural tension reinforcement

β - the ratio of distance between neutral axis and tension face to distance between neutral axis and reinforcing steel with a usual value of 1.2:

$$\beta = \frac{h-x}{d-x} = \frac{h-kd}{d(1-k)} \tag{2}$$

Where: $k = c/d = x/d$, is the ratio of distance between neutral axis and the compressive area of concrete. Equation (1), was adopted by ACI 440.1R -01 and ACI 440.1R -03 where a coefficient kb , was included to take account the bond properties of GFRP bars with concrete:

$$w = 2.2 \cdot \beta \cdot \epsilon_f \cdot k_b \sqrt[3]{d_c \cdot A} \tag{3}$$

ACI 440.1R -06 calculated the maximum crack width following Frosch (1999), based on a real model rather than an empirical one. The formula is independent from the type of reinforcement (steel or FRP), but includes the coefficient k_b taking into account the bond properties of FRP bars with concrete:

$$w = 2 \frac{f_f}{E_f} \cdot \beta \cdot k_b \cdot \sqrt{d_c^2 + \left(\frac{s}{2}\right)^2} \tag{4}$$

w – maximal crack width (in. or mm).

f_f - the stress in GFRP reinforcement (psi or MPa).

E_f - modulus of elasticity of GFRP bars (psi orMPa).

β - the ratio of distance between neutral axis and tension face to distance between neutral axis and reinforcing steel

d_c - the concrete cover measured from the centroid of tension reinforcement to the extreme tension face of the concrete (in. or mm).

s – the distance between GFRP bars (in. or mm).

For GFRP bars with similar bond properties to those of uncoated steel bars, $k_b = 1.0$. Inferior bond behavior implies $k_b < 1.0$, and vice versa $k_b > 1.0$.

2. Experimental testing of cracking behavior of gfrp –rc beams

This paper contains experimental data derived from laboratory tests conducted on four reinforced concrete beams with GFRP bars. The purpose of these tests is the observation of crack width of the beams under the action of two concentrated loads and the comparison with theoretical predictions.

The cross-section of the beams is 250 X 400 mm, with 4000 mm span length, and 4200 mm total length. Concrete grade C30 is used. The concrete mix design and the mechanical properties of concrete and GFRP bars, are detailed in Table 3 and Table 4.

Table 3. Mix design of the concrete

| Tested beams | | | | |
|----------------------|-------|-------|-------|-------|
| Components | T1 | T2 | T3 | T4 |
| Concrete volume (m3) | 0.461 | 0.461 | 0.461 | 0.461 |
| Cement (kg) | 161.4 | 161.4 | 161.4 | 161.4 |
| Filler (kg) | 89.9 | 89.9 | 89.9 | 89.9 |
| Sand (kg) | 450.6 | 457.2 | 454.9 | 459.2 |
| Gravel (kg) | 291.2 | 291.2 | 291.2 | 291.2 |
| Water (liters) | 59.6 | 56.3 | 57.6 | 56.6 |
| Additives (liters) | 3.23 | 3.23 | 3.23 | 3.23 |
| Ratio W/C | 0.37 | 0.35 | 0.356 | 0.35 |

Table 4. Mechanical properties of GFRP bars

| Diameter | | Cross section | | Weight | Modulus of elasticity E_f | | Tensile strength f_{fu}^* | | Ultimate elongation ϵ_{fu}^* |
|----------|---------|----------------------|----------------------|----------|-----------------------------|---------------------|-----------------------------|-----|---------------------------------------|
| SI (mm) | US (in) | A (mm ²) | A (in ²) | W (g/ml) | GPa | ksi 10 ⁶ | MPa | ksi | % |
| 15.875 | 5/8 | 197.9 | 0.307 | 181 | 46 | 6.7 | 620 | 90 | 1.42 |

The so-called "Ω" (Resistive displacement transducers) and horizontal LVDT (Linear Variable Differential Transformer), are used to measure the cracks width, while vertical LVDTs are used to measure the deflections of the beams. They are placed in areas where cracks are expected to appear, such as near the stirrups, being the area where the concrete is less homogeneous. In order to detect the cracks and later measure them, it must be located within the area of the arc of "Ω" in the concrete beam (approximately 5 cm), as in Fig. 2.

The tests would be carried out on four beams with different reinforcements. In the first pair of beams (beams T1 & T2), 4 Ø16 GFRP bars were used as longitudinal reinforcement, in the third beam (beam T3), 5 Ø16 GFRP bars were used as longitudinal reinforcement, and in the fourth beam (beam T4), 2 Ø16 GFRP bars were used as longitudinal reinforcement, while the upper reinforcement and staffs were not changed (Fig. 3).

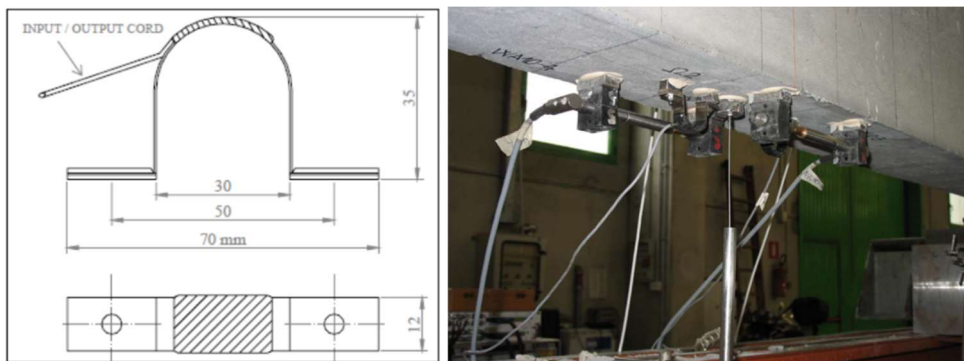


Fig. 2. Schematic view and positioning of resistive displacement transducers ("Ω")

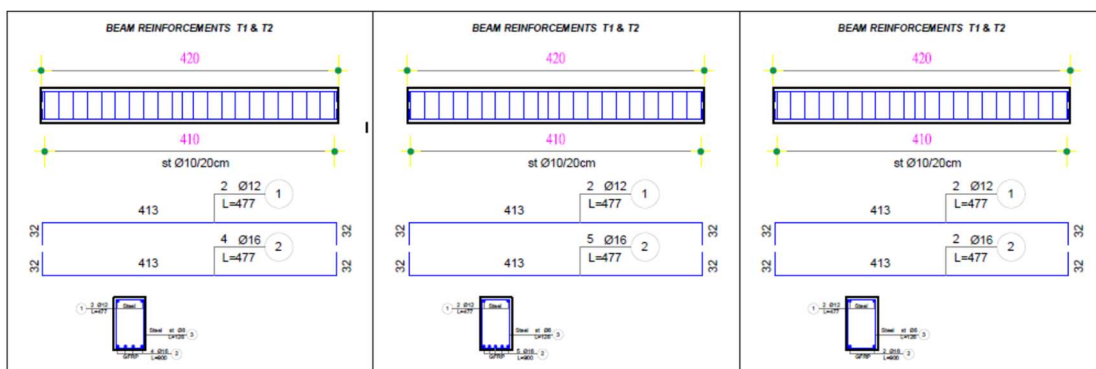


Fig. 3. The reinforcement of beams

Loading is done in cycles by scaling the electronic press at a loading rate of 300N/second. The first loading cycle was taken up to 10 kN, the second up to approximately 30 kN, the third cycle up to approximately 60 kN and the last cycle up to the failure of the beam. Only in the T4 beam, this loading is done initially up to 10 kN, then up to 20 kN, up to 40 kN until the beam failure [12].

After each cycle, the loading was stopped and kept constant in order to mark with a pencil the cracks visible to the naked eye and by photographing it, creating a complete framework of the crack development in the beams until their destruction. The data related to the size of the cracks, the reductions and the curvature of the beam as a function of loading, are recorded by the MGC device and elaborated in the form of graphs.



Fig. 4. Beam T1 & T2 - Concrete crushing failure, full cracked section (≈ 90 kN) [12]



Fig. 5. Beam T3 (≈ 102 kN), T4 (≈ 55 kN)-Concrete crushing failure, full cracked section [12]

3. Experimental testing of cracking behavior of gfrp –rc beams

This paper contains experimental data derived from laboratory tests conducted on four reinforced concrete beams with GFRP bars. The purpose of these tests is the observation of crack width of the beams under the action of two concentrated loads and the comparison with theoretical predictions.

Experimental data are analyzed and integrated in appropriate curvatures and are compared to theoretical calculations based on American Code ACI 440.1R -06.

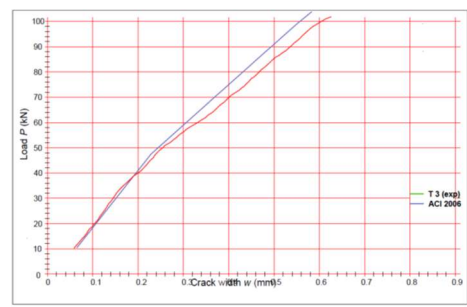
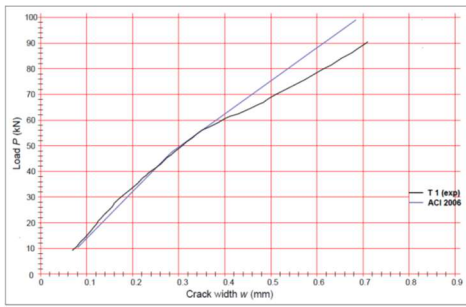


Fig. 6 Experimental vs predicted maximum crack width of T1 & T2.

Fig. 7 Experimental vs predicted maximum crack width of T3.

At the first pair of beams T1 & T2 were used 4 bars Ø16 GFRP, as longitudinal reinforcement with a theoretical balanced reinforcement ratio of $\rho_b = 0.00932 \approx \rho_{fb} = 0.00932$.

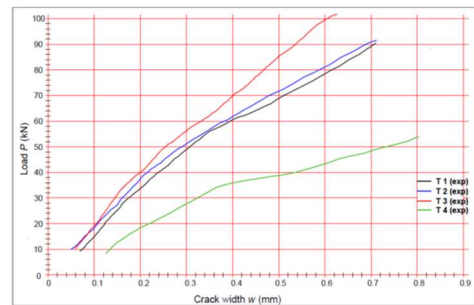
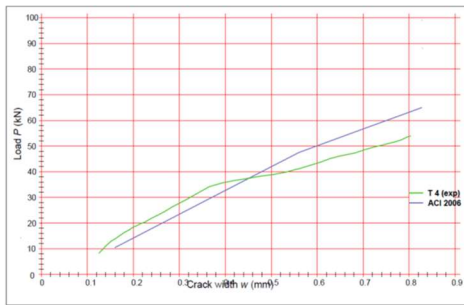


Fig. 8 Experimental vs predicted maximum crack width of T4

Fig. 9 Experimental maximum crack width of T1, T2, T3, T4

At beam T3 were used 5 bars Ø16 GFRP, as longitudinal reinforcement, having a lightly overreinforced beam where: $\rho_b = 0.0093 < \rho_f = 0.0116 < 1.4 \rho_{fb} = 0.013$.

At beam were used 2 bars Ø16 GFRP, as longitudinal reinforcement, having an underreinforced beam where: $\rho_f = 0.00466 < \rho_{fb} = 0.0093$.

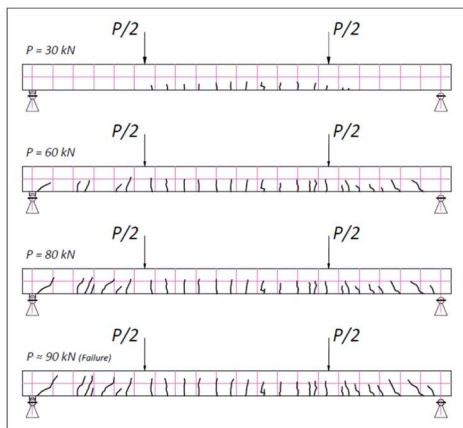


Fig. 10 Crack pattern of beam T1 in different phases of loading.

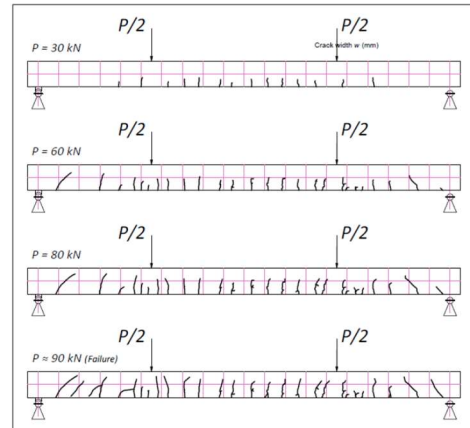


Fig. 11 Crack pattern of beam T2 in different phases of loading.

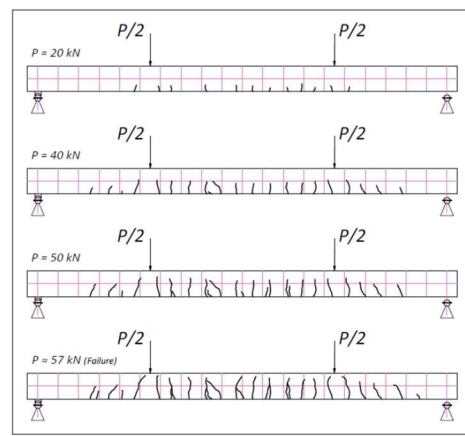
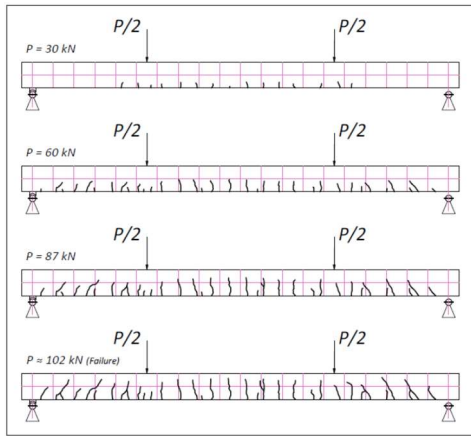


Fig. 12 Crack pattern of beam T3 in different phases of loading.

Fig. 13 Crack pattern of beam T4 in different phases of loading.

At beam T1 & T2, the maximum crack width $w_{max} = 0.7$ mm, is reached at the same time with beam failure from concrete crushing for $P \approx 89$ kN. Both beams show the same behavior in cracking width so the charts are quite superposed with indifferent discrepancies. Initially up to $P = 60$ kN, the chart of theoretical predictions is similar and superposed with the experimental one, but later on, it shows 11-12% smaller values than experimental results.

At beam T3, the cracking pattern and their development is similar to T1 & T2, but the failure happens for $P = 101.5$ kN and $w_{max} = 0,61$ mm or 12-13 % lower than T1 & T2. Initially up to $P = 60$ kN, the theoretical predictions is similar with the experimental results, but later on, it shows 7-8 % smaller values than experimental results.

At beam T4, the initial cracks are rare. The failure happens for $P = 56.9$ kN and $w = 0.81$ mm, so much bigger than the limit of $w_{max}=0.7$ mm, and the beam is out of service before concrete crushing. The crack width is 140% higher than T1 & T2. The theoretical predictions up to $P=40$ kN, are 15% higher than experimental results. After this moment, they are 20% lower than experimental results so we have discordance.

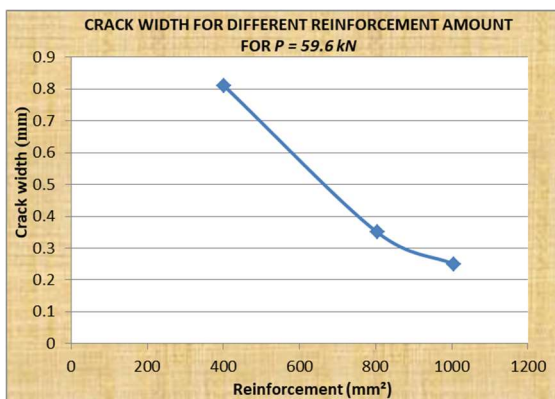


Fig. 14 Beam crack width – reinforcement ratio at rupture load of T4

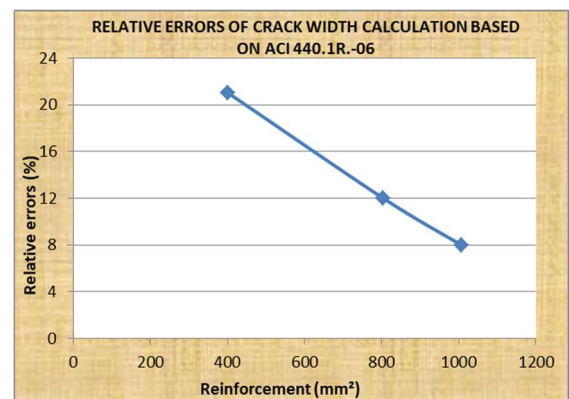


Fig. 15 Relative errors of crack width – reinforcement ratio (ACI 440.1R.-06)

Fig. 14 shows the beam crack width – reinforcement ratio at rupture load of T4 for $P = 56.9$ kN. The greater the reinforcement, the smaller the crack widths, and this goes almost linearly in inverse proportion. The error tends to decrease almost proportionally with the beam reinforcement increment as shown in Fig. 15, and this is similar to steel reinforced beams.

III. CONCLUSIONS

After experimental results analysis and their comparison with the theoretical predictions based on ACI 440.1R.-06, we can summarize the most relevant conclusions as follows:

1. The cracks start since the first phase of beam loading (30 kN), but still can't be seen with the naked eye. The cracks start

near the supports and the stirrups, and after they point toward the acting loads. In GFRP reinforced concrete beams, when they have a balanced reinforcement ratio, or when they are lightly over-reinforced, the maximum crack width of 0.5-0.7 mm, is reached at the same time with the flexural beam failure, except for the under-reinforced beam where the opposite occurs, due to GFRP bars rupture.

2. For the same loading level in the under-reinforced beam the crack width is 2.5-3 times larger than in the other beams, due to the lower reinforcement ratio.
3. During the comparison between theoretical predictions based on ACI 440.1R-06 and experimental results, was noted that this design code this code is not quite accurate for calculating the crack width with differences in the range of 8-21%, due to different reinforcement ratios, regardless any small problem during the tests.
4. Diversely from the deflections, the crack width has the trend to have bigger errors of the theoretical predictions, with the decrease of reinforcement ratio, so their curvature is inversely proportional.

Although the expectation based on theoretical predictions was appropriate (except for beam T4), these specimen tests were not enough to carry out important remarks for improving the design equations for calculating deflections and crack width of GFRP reinforced concrete beams and are needed more research.

REFERENCES

- [1] Abdul Rahman MS., Narayan SR. "Flexural behavior of concrete beams reinforced with glass fiber reinforced polymer bars". *J Kejuruteraan Awam* 2005;17(1):49–57.
- [2] ACI Committee 318. ACI 318R-05. Building code requirements for structural concrete (ACI 318-11) and commentary (ACI 318R-11). Farmington Hills, Mich., USA: American Concrete Institute (ACI); 2011.
- [3] ACI Committee 440. ACI 440.1R-06, Guide for the design and construction of concrete reinforced with FRP bars. Farmington Hills, Mich., USA: American Concrete Institute (ACI); 2006.
- [4] Al-Sunna Raed., Pilakoutas K., Hajirasouliha I., Guadagnini M., Deflection behaviour of FRP reinforced concrete beams and slabs: an experimental investigation. *Compos Part B Eng* 2012;43(5):2125–34 [Online publication: 1-Jul-2012].
- [5] Barris, P. C., Llinas, Ll. T., Serviceability behaviour of fibre reinforced polymer reinforced concrete beams [Ph.D. thesis]. Girona, Catalonia, Spain: University of Girona; 2010.
- [6] Benmokrane, B., Chaallal, O., Masmoudi, R., (1996a), Flexural response of concrete beams reinforced with FRP reinforcing bars, *ACI Structural Journal*, Vol. 93, No. 1, pp. 46–55.
- [7] Fatih, K. I., Ashraf, A. F., Flexural performance of FRP reinforced concrete beams. *J Comp Struct* 2012;29 [Available Online 29 December 2011].
- [8] Deneko, E. "Use of FRP bars as internal reinforcement in concrete members", Doctorate thesis in Civil Enginnerin, Polytechnic University of Tirana, 2017.
- [9] Faza, S. S., and GangaRao, H. V. S.,(1993), Theoretical and experimental correlation of behavior of concrete beams reinforced with fiber reinforced plastic rebars, in *Fiber-Reinforced-Plastic Reinforcement for Concrete Structures*, SP-138, American Concrete Institute, Farmington Hills, MI, pp. 599–614.
- [10] Nanni, A. (1993a), Flexural behavior and design of reinforced concrete using FRP rods, *Journal of Structural Engineering*, Vol. 119, No. 11, pp. 3344–3359.
- [11] Shanour, S. A., Behavior of concrete beams reinforced with GFRP bars [Ph.D.dissertation], Faculty of Engineering, Shoubra, Benha University, Cairo, Egypt; due 2014.